



Contextualized indicators for online failure diagnosis in cellular networks



Sergio Fortes, Raquel Barco*, Alejandro Aguilar-García, Pablo Muñoz

Universidad de Málaga, Andalucía Tech, Departamento de Ingeniería de Comunicaciones, Campus de Teatinos s/n, 29071 Málaga, Spain

ARTICLE INFO

Article history:

Received 13 June 2014

Received in revised form 2 December 2014

Accepted 4 February 2015

Available online 4 April 2015

Keywords:

Self-healing

Diagnosis

Context-aware

Localization

Small cells

LTE

ABSTRACT

This paper presents a novel approach for self-healing in cellular networks based on the application of mobile terminals context information: time, service, activity, identity and, especially, location. Context information is therefore used to support root cause analysis, providing improved network fault diagnosis compared to classical non-context-aware approaches. The integration of context information is implemented by means of the newly defined contextualized indicators. These are used in order to integrate user equipment context information in pre-existent failure management schemes. The presented techniques are especially suitable for indoor small cell scenarios, whose particular conditions of dynamic user distribution, overlapping coverage, dynamic radio and service provisioning environment, etc., make previous diagnosis schemes especially unreliable. The algorithms and methodology for the proposed context-aware system are defined and its performance is assessed by means of an LTE system-level simulator.

© 2015 The Authors. Published by Elsevier B.V. This is an open access article under the CC BY-NC-ND license (<http://creativecommons.org/licenses/by-nc-nd/4.0/>).

1. Introduction

Troubleshooting is one of the most time and resource-consuming tasks in cellular network operations. Faults in network elements (e.g. in base stations, backhaul, etc.) often end up requiring field engineers and/or technicians visits to the site, which introduce high expenditures. Base stations are extremely complex systems, composed of multiple and redundant equipment, from the power supply to the pure communication subsystems. The lack of a proper knowledge of the causes of a failure can easily lead to high delays in fault recovery. This may include multiple visits to the site and/or long system monitoring time, with the corresponding costs and disruption of the user service, which strongly impacts the operator brand image.

Operators and standardization bodies have proposed different approaches to reduce these expenditures by means of automating network failure management. In this field, the Next Generation Mobile Networks (NGMN) Alliance [1] and the 3rd Generation Partnership Project (3GPP) [2] defined the Self-Organizing Networks (SON) concept [3]. SON encompasses three main areas of cellular system operations, administration and management (OAM): self-configuration, the initial automatic configuration of the network elements; self-optimization, the tuning of network parameters to adapt the system to changes; and self-healing, the automatic identification and correction of network failures.

Self-healing consists of fault detection, root cause analysis (diagnosis), compensation and recovery. In spite of being one of the key factors to keep the quality of service (QoS), self-healing has been scarcely analyzed in the literature, partly due to the intrinsic difficulties of network failure identification in such a complex system as a cellular network.

* Corresponding author.

E-mail addresses: sfr@ic.uma.es (S. Fortes), rbm@ic.uma.es (R. Barco), aag@ic.uma.es (A. Aguilar-García), pabloml@ic.uma.es (P. Muñoz).

On the one hand, new challenges greatly impact the application of self-healing in current deployments. Cellular infrastructure consists in heterogeneous networks (HetNets). These are characterized by the simultaneous coexistence and interaction of multiple radio access technologies (RATs) such as GSM, UMTS, LTE (Long-Term Evolution) and different cell station deployment models (e.g. femtocells, picocells, etc.). HetNets complexity leads to an increased demand for automatic, fast and accurate diagnosis mechanisms.

On the other hand, the wide market penetration of smartphones and tablets (about the 74% of mobile terminals [4]) enlarges the amount of distributed sensing and computational capacity in the network. New mobile terminals are powerful platforms highly equipped with sensors and applications that increase the availability of terminals and users' *context information* [5]. Context encompasses information on the user conditions such as location and activity, opening the opportunity to make use of this data for network diagnosis purposes.

In this way, *user equipment* (UE) data can be included as a new source of information for self-healing, where such solutions are especially promising in the field of indoor deployments of small cells. Small cells are low powered base stations aiming to provide specific coverage to certain spots and increasing frequency reuse [6]. Their deployments are characterized by overlapping cell coverage areas (between small cells and with the macrocells). Also by highly variable distributions of the UEs, as the reduced coverage areas (in the range of dozens of meters) allow fast variations in cell occupation. Furthermore, small cell networks are commonly more prone to failures as they are often more accessible to unintentional or intentional damage and rely on vulnerable infrastructure: especially femtocells, which make use of common broadband connection and routers. All these characteristics make small cell networks especially predisposed to failures that may stay undetected for long periods of time.

In this respect, UE context data related to the users' services, activity, consumption, applications and, especially, location would be an invaluable source of support to overcome the described challenges for self-healing at indoor scenarios. This work is focused on the definition, description and assessment of the novel concept of contextualized indicators to integrate such information into existing diagnosis mechanisms, highly increasing their accuracy.

This work is organized as follows: Section 2 presents the general problem formulation, as well as the literature review and the contributions of this work. Section 3 defines the mathematical processes related to the generation of contextualized indicators. Section 4 integrates the contextualized indicators into a complete diagnosis scheme. Section 5 assesses the challenges related to performance indicator generation and establishes three main approaches to deal with the possible lack of samples for their calculation. Section 6 shows the results of evaluating the presented mechanisms in an LTE system-level simulator modeling a key indoor scenario. Finally, Section 7 presents the conclusions of the work.

2. Problem description

In the analysis of network performance, a *problem* is defined as a degradation in the service provision [7], e.g. dropped calls, while the *fault* or *cause* refers to the specific software or hardware issue that generates the problem. Problems are commonly defined at cell level, even if they may be located at other levels of the infrastructure such as at the operator's core and the backhaul.

If a cell has a problem, it is categorized as *problematic*. Depending on the origin of the failure, a cell can be also categorized as *faulty*, if it provokes the cause/fault of the problem; or *victim* if the cell itself does not generate any fault but it is affected by other faulty cells. For example, a victim cell can be overloaded by the traffic coming from the outage of another close cell. Victim cells are usually adjacent neighboring cells to the faulty one but not necessarily, as shown in Fig. 1. For example, a cell can suffer interference coming from distant base stations transmitting at high power in the same frequency band.

In this field, root cause analysis consists of the diagnosis or identification of the specific *cause* generating a problem. This step is essential to select and execute the necessary actions to compensate for and/or recover the network from the fault. Root cause analysis has been commonly based on the correlation and statistical analysis of different sources of information gathered from faulty and/or victim cells and their associated infrastructure. In this respect, the main sources of information are:

- *Alarms*: automatic fault event messages generated by network elements.
- *Mobile traces*: measurements gathered from specific users or operator's test terminals.
- *Network counters*: radio measurements periodically reported to the OAM system by network elements.
- *Key performance indicators – KPIs*: combinations of multiple counters.
- *Status monitoring*: continuous (periodical or by demand) collection of information related to the status of a network element, commonly bases stations, e.g. heartbeat signals.

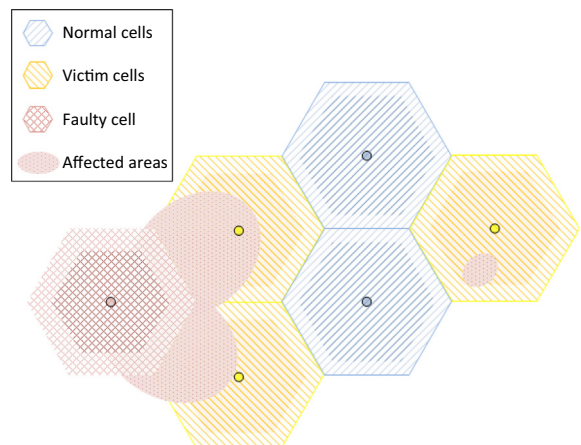


Fig. 1. Faulty/victim cell example.

Additionally to the presented sources of information, NGMN and 3GPP have recently identified the concept of SON enablers as additional inputs for failure management [8]:

- *Performance Management and Direct KPI Reporting in Real-Time*, which allows to gather statistics, alarms and cell data within very short time intervals (min/s).
- *Subscriber and Equipment Traces*, which define mechanisms for monitoring particular network elements or terminals for a certain period of time.
- *Minimization of Drive Tests (MDT)*, which enriches previous trace mechanisms by adding localization information to the UE reports. Here, UE positions are estimated by means of cellular techniques, e.g. timing advance, or global navigation satellite systems (GNSS).

Originally, root cause analysis was mainly based on alarm correlation. However, very often the same alarms can be triggered by different failure causes, therefore reducing their usability for fault identification. Additionally, a problem may not activate any explicit alarm. This makes the analysis based on other information sources (network counters, KPIs, status monitoring and mobile traces) essential for failure diagnosis analysis. All those sources will be indistinctly referred as *indicators* hereafter.

2.1. Classical indicators

Based on the presented sources of information, the classical mechanism for network monitoring is presented in Fig. 2 left column. In such an approach, the performance analysis is based on indicators at cell level, k^M , where k refers to the specific indicator and M is the set of measurements from which is calculated. The majority of these indicators are generated by statistical analysis of the

measurements and/or event-related counters coming from the UEs in the serving cell. For example, the call drop ratio of the cell, the Xth-percentile of the UE received power, etc. Particularly, the indicators related to measurement reports are calculated based on statistics of the received UE samples (e.g. $m'(u_i, t)$ from the UE u_i at instant t).

In this classical view, the set of samples used for calculating a value of the indicator depends uniquely on the period of time when they were gathered and the serving cell of the reporting UEs. The process is classically transparent for the network operator, the indicators being automatically generated by the OAM system, providing in consequence a value of $k^M[n]$ for each observation period n , for example each hour.

In small cell networks, one of the main issues of using classical indicators for diagnosis is the highly overlapped coverage areas. This might lead to a failure not being significantly reflected in the statistics depending on the distribution of the UEs. For example, the problem may stay hidden for the operator till a specific UE spatial distribution and/or traffic demand (peak hour) provokes an explicit degradation in the network service. However, the problem should be averted in advance to avoid its impact on network service provisioning.

Additionally, the small coverage areas can easily lead to a low number of UEs per cell and fast changes in their distribution. This can result in lack of data for the indicator calculation or drastic variations in the statistics. In the future, such an issue will become even more critical, as SON functions are expected to reduce their response time from the classical hours to min/s in order to provide fast response to network issues [9].

The use of direct information at the UE level could help to overcome those issues. Classically these reports are obtained from particular UEs by subscriber traces, drive test, MDT or over the top applications. Such information allows analyzing the service performance of specific

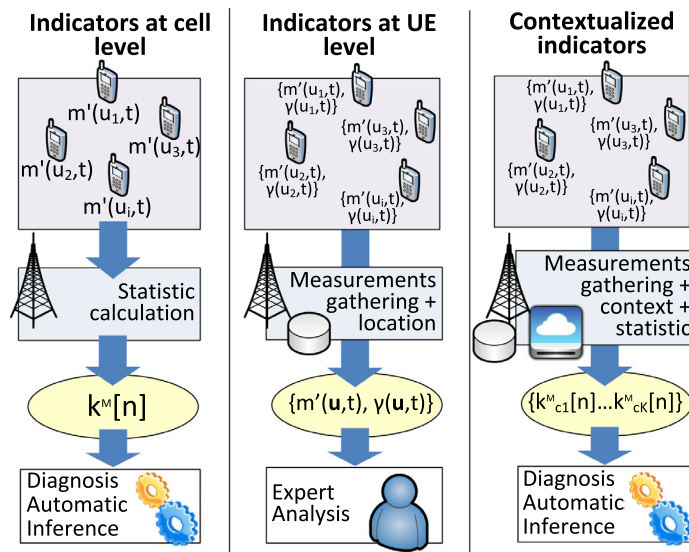


Fig. 2. Classic and proposed contextualized approaches for KPI generation mechanisms.

terminals, where the indicator can be enriched with additional context information, typically the UE location obtained in drive tests and MDT. However, as represented in Fig. 2 central column), the analysis of the context of such data has been till now mainly based on human expert analysis, which is extremely time consuming. Also, the manual approach lacks the required automation for fast response to network failures.

2.2. Related work

To improve the presented situation, an automatic approach for using context information in diagnosis is deemed indispensable in current OAM systems, especially given the growing demand of complex cellular infrastructure.

However, until now, studies in self-healing have mainly centered their analysis in macrocell scenarios. Refs. [7,10] proposed general frameworks for self-healing procedures in such environments, establishing the bases for the use of KPIs for diagnosis purposes.

Refs. [11,12] defined further refinements in the treatment of the indicators in detection and diagnosis, incorporating procedures to model different failure causes and comparing them with real time current network states. However, no context information was included in those studies.

The idea of using direct UE reports can be considered in line with the works on MDT, recently incorporated to the standard [13,14]. As previously explained, in MDT the UEs report special measurement messages that include, when possible, localization information. Such localization is roughly estimated by cellular based methods (e.g. timing advance, propagation delay, etc.) or GNSS. However, MDT approaches mainly address offline performance analysis of the network and no previous work has presented a systematic approach for incorporating this information to online diagnosis in indoor small cell environments.

Some mechanisms could be used for the integration of context information into the analysis of network performance. Ref. [15] included the UE position as an additional parameter for generating macrocell diffusion maps for sleeping cell detection. Ref. [16] suggested the use of a semantic reasoner and clustering map in the field of general telecommunication service adaptation. However, such mechanisms did not provide a numerical straightforward indicator on network performance, implying the modification of current network monitoring procedures. Therefore, its adoption in current systems is not evident.

Ref. [15] proposed the use of diffusion maps (a data mining technique) for detection of the *sleeping cell* problem. While that work used simulated positioning information of the UE, it did not elaborate on the comprehensive application of such information, also focusing the analysis only on an elementary reference macrocell scenario and a very limited set of network problems.

Additionally, previous work of the authors [17] proposed a location-aware architecture that could partially support OAM context-based functionalities. However, this work only presented a self-optimization showcase technique. Also the tutorial work presented in [18] defined a

general framework for context-aware self-healing and indicated the general conditions for its application in small cell scenarios. However, no comprehensive methodology was included and just a showcase mechanism for cell disconnection was proposed.

2.3. Proposed solution

Therefore, a lack of comprehensive developments in the field of cellular network failure management based on context information has been identified. However, the use of context information has been considered useful for self-healing and, therefore, it is analyzed in this work. Thus, this paper presents a novel approach for integrating context information into self-healing. This is achieved by means of contextualized indicators, which combine radio performance measurements and UE context information. These indicators will have the advantage of being easy to integrate in current diagnosis mechanisms. In terms of the considered evaluation scenarios, the proposed approach can be applied indistinctly for macro and small cell environments. This paper will be focused on indoor small cell scenarios, these being the more challenging from a self-healing perspective, and therefore those that could benefit the most from the proposed developments.

Here, the main contributions of this work are: firstly, the definition of the contextualized indicator approach as a way to introduce context information into current self-healing mechanisms for cellular networks; secondly, the mathematical formulation of such an approach in a comprehensive manner that allows the definition and application of any particular set of context sources by defining context masks; thirdly, the integration of these contextualized indicators into a diagnosis scheme; fourthly, the analysis of the implications of the proposed approach from a computational and architectural way and from the perspective of both consumers and operators; and fifthly, the assessment of the proposed approach by a particular example of context mask based on location, evaluating the capabilities of the approach for a key simulated scenario. This approach can be applied for macrocell and small cell scenarios alike. However, its evaluation will focus on the small cell case, being one of the most challenging environments that could benefit from the approach.

3. Contextualized indicators

This paper proposes the construction of *contextualized indicators* for network analysis, where both UE radio measurements and context are used to generate the indicators. In order to do so, the mathematical expressions related to such indicators are defined. This way, a contextualized indicator $k_c^M[n]$ is defined as:

$$k_c^M[n] = \varphi_c^M(\{m'(u_i, t_z), \gamma(u_i, t_z) | u_i \in U_{sc}, t_z \in T_n\}), \quad (1)$$

where the contextualized statistic φ_c^M is calculated based on both measurements $m'(u_i, t_z)$ and their related context $\gamma(u_i, t_z)$. Here, u_i refers to a specific UE of the set of network reporting terminals, U_{sc} . Contrary to classic indicators at cell level, these UEs do not have to be served by a unique

cell. t_z represents the instant of measurement in the observation period T_n .

The context of one UE is composed of different categories and values, such as location, user category and service conditions:

$$\gamma(u_i, t_z) \sim \{x(u_i, t_z), y(u_i, t_z), z(u_i, t_z), sc(u_i, t_z), \dots\}, \quad (2)$$

where x, y, z represent the position of the UE when the measurement was gathered and sc indicates the serving cell. Many more context parameters can be defined, such as current demanded quality of service, trustfulness in the terminal report, terminal orientation and speed. Some of this context information can be directly received from the terminal or they may be estimated from other parameters. For example, UE speed, if required, may be calculated from previous position reports.

This method greatly differs from that presented in [18], where the measurements of each particular terminal are analyzed based on historical positioned data. Hence, a certain period of time would be required to start generating meaningful data about each UE. This makes that approach more dependent on the recorded database of previous samples and on the mobility of each terminal.

3.1. Statistics calculation

Once the collection of measurements and context for a certain period has been obtained, how to generate the contextualized statistic φ_c^M should be defined. This paper proposes the use of *sample weights* for this task.

Sample weights are a concept applied in the field of population statistics and social polling [19]. In social polling, sample weights are mainly used to tame the effect of heterogeneous sampling likelihood of a particular population group. However, they have not been, to the best of the authors' knowledge, previously applied in cellular networks monitoring.

In order to have a comprehensive way to calculate any desired statistics from both measurements and context, the sample weights concept is applied to the calculation of the empirical probability density function (epdf) [20] of the UE measurements.

In the proposed approach, sample weights are used as a way of increasing the impact of some measurements compared to others on a certain contextualized indicator. This concept is based on the idea that the reports gathered under certain context (e.g. from a specific area, or terminal) would have higher relevance in the detection and

diagnosis of certain failures. Based on this premise, the epdf for a specific contextualized indicator can be calculated as:

$$\hat{p}_c(m)|_{M'} = \frac{1}{A_w} \sum_{m' \in M'} \delta(m - m'(u_i, t_z)) \cdot w_c(\gamma(u_i, t_z)), \quad (3)$$

where $w_c(\gamma(u_i, t_z))$ represents the weight related to the context $\gamma(u_i, t_z)$ of a certain measurement $m'(u_i, t_z)$. The expression is normalized dividing it by A_w , representing the sum of all the weights applied $W_c(M')$ to the set of measurements M' . Therefore, weights will have an impact on the original probability distribution of a certain indicator by giving higher or lower importance to some samples.

The epdf can be used as the base for approximating an underlying parametric (Gaussian, beta, etc.) or non-parametric distribution of the measurements (see Fig. 3). From such a distribution, the particular statistic φ^M (as the mean, Xth percentile, variance, etc.) can be calculated to generate the indicator values $k^M[n] = \varphi^M(\hat{p}(m)|_{M'})$.

3.2. Weight masks

To simplify weights calculation and increase their applicability, the *context masks* concept is also introduced. A context mask defines a relation between a particular context attribute and a set of weights. For example, a location mask may define sample weights as inversely proportional to the UE distance to the serving base station. In the same way, a service mask can consist in discarding (weight 0) all terminals that have no visibility (no received signal) from a certain cell.

Also different context masks could be defined for the same context attribute. Hence, a context mask could apply lower weights to samples far from the cell station position, increasing the importance of close samples for issues related to the base station proximity. Conversely, another mask could define a higher weight for positions close to the external walls/windows of the building, thereby increasing the importance of border effects.

The multiple context masks contribute to the *total weight* ($w_c(\gamma(u_i, t_z))$) applied to each sample. This can be defined as a function ϕ_c of the multiple weights generated by the simultaneously applied context masks (see Fig. 5):

$$w_c(\gamma) = \phi_c\left(\left\{w_c^{p1}(\gamma_{xyz}), w_c^{p2}(\gamma_{sc}) \dots\right\}\right), \quad (4)$$

Each combination of context masks implies the generation of a particular contextualized indicator, as represented in Fig. 4. In this figure, the top part reflects the classic

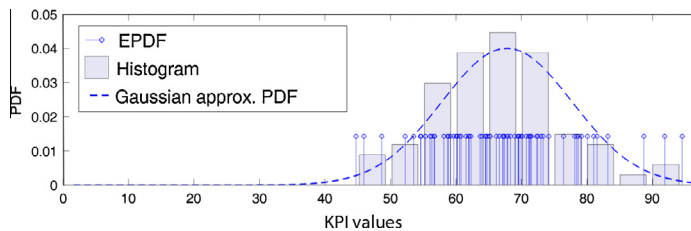


Fig. 3. Empirical pdf, histogram and associate approximate normal distribution.

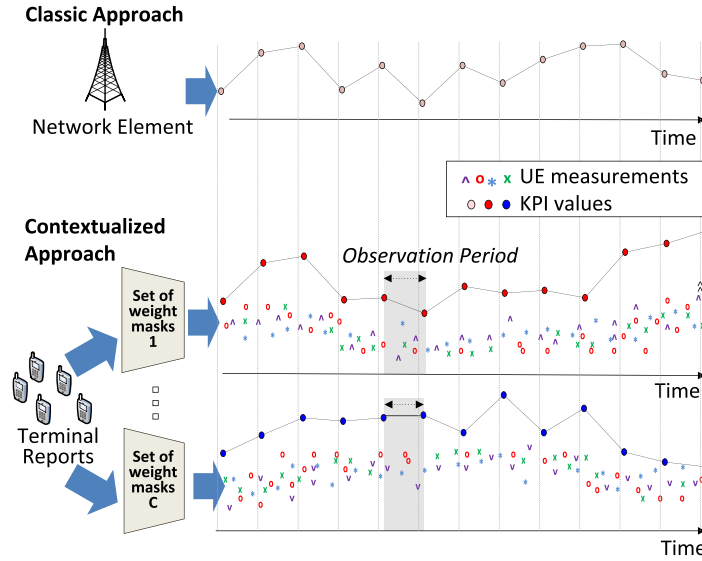


Fig. 4. Classic and proposed approached for the diagnosis inference mechanisms.

approach, where one indicator is directly generated by a network element (e.g. base station) in a transparent way. In the proposed approach (bottom) different contextualized indicators can be calculated depending on the set of context masks applied to the UE measurements. In this case, each indicator value is computed based on the weighted UE measurements received during an observation period.

3.3. Binary weights

The weights of a context mask can be specified as any function of the context attributes. As a useful option, the use of binary weights, which can only have a value of 0 or 1 for any particular context, is proposed:

$$w_c^p(\gamma) = \begin{cases} 1 & \text{if } w_c^p \text{ conditions for } \gamma \text{ are met} \\ 0 & \text{otherwise} \end{cases} \quad (5)$$

This is equivalent to discard or accept certain samples depending on their compliance to a given condition. For example, if the position of the terminal is inside a certain area. This solution is good in terms of simplicity and fast computation, but it eliminates the possibility of finer weights (e.g. gradual increase in the weight of a sample depending on its distance to a base station).

This approach is especially useful for context masks based on *geographical areas*. This way, just the samples measured in certain regions can be included in the calculation of a contextualized indicator. The cell center, its edge, the building border, etc., are areas whose statistics are especially interesting for diagnosis purposes. Binary weights are also appropriate for selecting samples obtained from terminals served just by specific cells or meeting certain conditions.

For the generation of the total weight, ϕ_c can still be freely defined by any combination of the different weight masks. However, if only binary weights are used, these can be easily combined by logical operators such as AND

and OR. The total weight can therefore define the intersection or the union set of measurements satisfying different context masks.

For binary weights, the calculation of the epdf would not be required to obtain any context statistics, as these can be calculated directly over the original samples M' by simply discarding the measurements with total weight equal to 0, reducing the computational costs of the process.

4. Context-aware diagnosis

Once the contextualized indicators have been defined, they have to be integrated in the diagnosis process. Here, a diagnosis scheme based on a naive Bayes classifier is presented and adapted.

Such a mechanism, as well as any statistical based diagnosis system, requires a *learning phase*, where the system adapts to the network conditions and its expected outputs under different network states. Then, the system is used for the diagnosis of failures causes during the *diagnosis phase*.

4.1. Learning phase

For the diagnosis of the specific failure cause, the current values of the indicators have to be compared with the *statistical models* of the indicators. These models are constructed during the *learning phase*.

Following the framework presented in [7], models consist of the estimated *conditional probability* of each indicator value given a certain *network state*: a normal status or a specific failure cause. The expression for a contextualized indicator is:

$$P(K_c^M | S = s_i), \quad (6)$$

where $P(K_c^M | S = s_i)$ is the approximate conditional probability for the values of the indicator K_c^M given a specific

network state $S = s_i$ (e.g. normal status, interference from a cell, etc.).

In order to calculate such a probability, the indicator values for different *labeled periods*, periods where the specific failure cause/state of the network is known, are gathered. Based on the equally labeled values of this training set, the conditional probabilities are calculated approximating their function by a parametric (e.g. Gaussian, beta) or non-parametric distribution (e.g. k-density, normalized histogram) [21].

4.2. Diagnosis phase

In the diagnosis phase, the failure cause affecting the network is identified by comparing the current indicator values to the models generated during the learning phase. In order to do so, the values of one or multiple KPIs shall be compared to the statistical profile generated in the learning phase for such indicators.

This comparison may be performed following different inference mechanisms. Here, a naive Bayes classifier is proposed as a baseline diagnosis method [21]. A naive Bayes classifier is based on the use of the Bayes' theorem assuming strong independence between the features. This classifier includes four main parameters:

- *Evidence*: known values of network indicators.
- *Prior probabilities* of each network state, this means the likelihood of the network being in a certain status if no evidence is known.
- *Conditional probabilities*: the probabilistic relation between the values of the features/indicators and a given network status.
- *Posterior probabilities*: the likelihood for a certain network state given the evidence and the conditional probabilities.

If contextualized indicators are used as inputs of the classifier, this can be expressed as:

$$P(S = s_i | \mathbf{K})_n = \frac{P(S = s_i) \prod_{k_c^M \in \mathbf{K}} P(K_c^M = k_c^M[n] | s_i)}{P(\mathbf{K})} \quad (7)$$

where $\mathbf{K} = \{k_{c1}^{M1}[n], k_{c2}^{M1}[n], \dots, k_{c1}^{M2}[n], \dots\}$ is the evidence, composed of the set of input KPI values in the n th observation period. Each of these KPIs can be based on different measurable parameters M and/or context masks c . $P(K_c^M = k_c^M[n] | s_i)$ is the conditional probability of the indicator input ($k_c^M[n]$), which is calculated from the models obtained in the learning phase. For a possible network state $S = s_i$, $P(S = s_i)$ indicates its prior probability and $P(S = s_i | \mathbf{K})$ represents its *posterior probability* given the evidence \mathbf{K} with probability $P(\mathbf{K})$. $P(\mathbf{K})$ being equal for all $P(S = s_i | \mathbf{K})$, this term can be discarded for comparisons between the probabilities of different states.

Eq. (7) can be applied assuming the independent computation of the probability distributions for each KPI, avoiding the calculation of multidimensional joint probability distributions that would be required if independence was not assumed. Although being a simple mechanism,

naive Bayes classifiers have demonstrated good performance in a huge variety of situations, even when independence between the features is not guaranteed [22]. Once the classifier returns the posterior probabilities, inference of the network state can be based on a simple maximum a posteriori (MAP) decision rule, consisting in selecting as the estimated network status $\hat{s}[n]$ the one with maximum posterior probability, which provides the results for the diagnosis method.

For this approach, each time the diagnosis system receives the values of the indicators for a period n , these are analyzed without considering previous or posterior samples. This allows to generate a diagnosis for each period with just one value of each considered indicator. Additional mechanisms making use of the time series evolution could also be used with contextualized indicators. For example, that presented in reference [12]. Here, an *observation window* is used for the most recent indicator values. However, such time series approaches may lead to an increase in the time needed by the algorithm to diagnose and also imply higher computational costs. Therefore, their application would be reserved to further studies.

4.3. Data scarcity avoidance

The use of context masks, especially binary ones, could lead to having not enough UE measurements to calculate a contextualized indicator. If there are not enough measurements that meet the conditions of an applied set of context masks (for example there are no users on the edge of a cell), the value of the contextualized indicator could not be calculated for the period.

That situation could occur also for classical indicators, for example if a cell does not serve any UEs for a period. However, as the context masks can impose more restricted conditions, this problem may become more serious. To reduce the impact of such situations, this work proposes three different approaches:

- *Discard indicator*: Avoid using the affected indicator for the period without samples. However, having less indicators for the classification may lead to a reduction in the diagnosis accuracy.
- *No diagnosis*: If one of the selected indicators as input of the classifiers has no value, the system avoids providing any diagnosis result. This reduces the risks of providing erroneous results, while increasing the periods without answer and possibly increasing fault response delay.
- *Fallback*: A substitute input for the naive Bayes classifier is selected for the periods where the primarily selected indicator has no value. This substitute can be another contextualized indicators or a classic indicator. In this way the system can keep providing diagnosis results while at the same time trying to maintain accuracy.

The choice between the three techniques would depend on the OAM requirements and limitations in terms of accuracy and capacity to process and store multiple models and indicators.

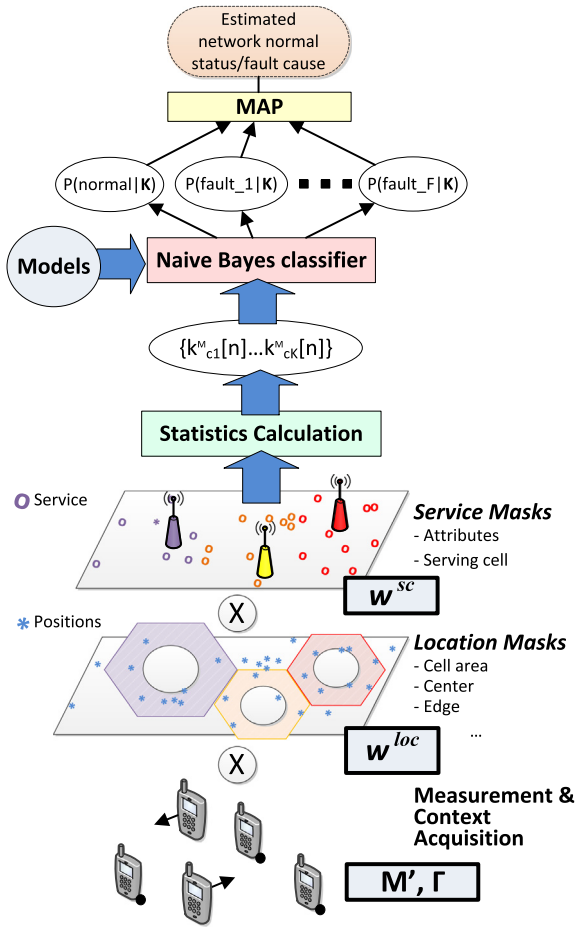


Fig. 5. Diagnosis data processing scheme.

4.4. Diagnosis scheme

The complete diagram of the presented approach is schematized in Fig. 5. Here, the network measurements M' and the collected context information for all terminals, $\Gamma = \{\gamma(u_1, t_1) \dots \gamma(u_i, t_i) \dots\}$, are processed by different context masks. In the represented scheme, different sets of location masks w^{loc} and service masks w^{sc} are applied, which leads to specific values for each contextualized indicators. Based on the correspondent models, the conditional probabilities for each possible network state are calculated.

As inputs for the classifier, the indicators where each state could be more easily distinguishable should be selected. These can be chosen based on the state models, by selecting those indicators where each model is more clearly differentiated from the rest. If the input indicators are already selected, only those have to be computed during the diagnosis phase (avoiding the calculation of other context mask combinations).

5. Implementation considerations

The presented mechanisms involve a series of requirements from an implementation point of view that would

highly impact their applicability in real cellular OAM systems. In this respect, the main considerations to take into account are at system level, or how the mechanisms can be located in a real OAM architecture. Also the available information as well as the computational complexity would highly impact the applicable context masks. This section addresses these issues, presenting some details for the real implementation of the proposed system.

5.1. System implications

In the proposed approach, the context information (and especially localization) may be obtained from different sources. On the availability of the localization information, multiple solutions and systems are commonly present for outdoor UE positioning. At the same time, indoor localization systems are becoming more extended, with multiple developed mechanisms based on cellular signal analysis [23] and other technologies also applicable for mobile terminals [24,25].

The OAM system can obtain this information directly from the operator network infrastructure (i.e. if cellular based localization is implemented) or the UEs, by means of management and/or control plane messaging [26]. It can also be obtained from UE user applications or external servers by over the top solutions (as the approaches proposed by [16–18]).

5.2. Hybrid and distributed approaches

The implications of distributed and hybrid approaches for self-organizing OAM systems in small cell environments have been analyzed by a recent work of the authors [17]. That paper presented the architectural characteristics of an integrated location-aware SON system dedicated to network optimization. It defined a hybrid local approach as the best way to avoid excessive backhaul traffic and computational costs. For such a solution, a local SON centralized unit is located on-site for a particular indoor small cell deployment (e.g. a mall), allowing the use of the proposed mechanisms without saturating the network backhaul, as well as being computationally manageable. Additionally, indicators based on a unique serving cell are particularly interesting for distributed approaches. Such indicators can be calculated by each cell itself if it has also access to the additional context information (from external sources through internet or directly coming from the terminal). This leaves the door open to hybrid implementations of mechanisms based on contextualized indicators. Moreover, pure distributed algorithms could be defined. For example, if a naive Bayes classifier is used, this can be implemented in a distributed manner. Each cell could calculate the conditional probabilities for their own served-based indicators. Then, these values can be shared between the cells to perform the multiplication required to obtain the final posterior probability of the network state.

5.3. Classifier inputs selection

For the classifier, its inputs need to be selected. In order to do so, common approaches make use of human

expertise in order to choose those that better reflect network failures [27].

For classical indicators, the options are limited, where the main indicators that can be used are those generated by the faulty cell and its neighbors. When more than one neighboring cell indicator is available, the one more affected by the failure could be chosen as input. In real environments, as the faulty cell is a priori unknown, all indicators would be monitored continuously.

For contextualized indicators, the choices grow exponentially, as multiple definable context masks can be applied, increasing the number of available indicators. However, a set of common location-based indicators can be straightforwardly defined for any environment, as they are clearly affected by different failures. The most useful indicators for each type of failure are presented below:

- *Small cell interference*: This kind of failure would particularly affect measurements gathered at the edge of the victim cell, closer to the interfering one.
- *Macro cell interference*: Such faults would especially affect the served edge of cells located in the border of the indoor location.
- *Power degradation*: In case a cell degrades its transmitted power, the most affected area would be the center of its expected coverage, even if no total coverage hole appears due to the overlapping coverage of other cells. The effects over classic performance indicators could be detected in the long run in dropped calls or excessive overload of neighboring cells. However, the indicated contextualized indicators should help to detect the fault before the service provision is affected.

These indicators can be applied to any deployment. In situations with multiple available indicators for each failure cause, that with the highest deviation with respect to the other network states would be selected. However, an analysis of other context mask options could also lead to the generation and selection of indicators providing even better performance.

5.4. Mask information sources

As defined in the previous subsection, location-based context masks associated with the center and the edge of a cell should be defined. To do so, different mechanisms can be established depending on the amount of information known on the scenario and the localization data precision:

- *Distance based*: if the distance of the UE to the base station is available or can be calculated, e.g. by means of time-of-arrival. This method is especially applicable for macro scenarios. However, it has been discarded for the analysis in this paper because indoor localization methods provide also coordinates, which allows to choose more precise masks.
- *Power diagram based – Voronoi*: Power diagrams are a generalized form of Voronoi tessellations based on the polygonal partition of the scenario taking into account the Euclidean distance between the base stations and

also their transmitted power [28]. This solution allows an estimation of the relative coverage areas and the expected serving cell for each point.

- *Propagation model based*: if enough data is known about the scenario (walls, obstacles and their attenuation), the radio coverage of the cells can be calculated by different propagation models, as in Winner II [29]. Considering shadowing effects may improve the estimated coverage areas. However, such calculations are computationally complex and require a degree of knowledge of the particular scenario that is far from the one that can be expected in real deployments. Also, such models can be highly impacted by changes in the scenario.
- *Measurement campaign based*: Also fingerprint measured information can be used to define the expected coverage area and the center of a cell. However, the need of test campaigns makes this solution not especially applicable if the fingerprinting information was not already obtained for other purposes, e.g. localization [30].

The choice of one or another solution would reside in the available information as well as the complexity of the scenario. In this respect, a power diagram based solution is assumed to be the best option in terms of computational cost and required inputs for open or semi-open areas. Additionally, Voronoi diagrams are very suitable for binary masks, where only the presence inside or outside one area would define the assigned weight 0 or 1. If propagation information is used instead, the same information can be the base to generate more complex weights, for example as functions of the expected received power.

5.4.1. Border effects

When using a location-based mask, and especially Voronoi based, the defined areas may encompass large zones outside the indoor scenario. This could lead to erroneous aggregation of UEs located outside the premises. Such a problem can be straightforwardly avoided if the indoor location perimeter is known. In such a case, the samples gathered outside the scenario can be weighted or discarded based on their position. Additionally, if particular weights are assigned to those samples, they can be used to perform analysis on the interference generated in the exterior by the small cells. In order to reduce the additional computation cost of applying this perimeter mask, other approach is possible: truncating the Voronoi-based areas by the intersection points with the scenario perimeter. The new calculated areas can then be applied directly during the diagnosis phase. Moreover, other context-based solutions can be also used to discard such samples. For examples conditions related to the unavailability of indoor localization, service that commonly stop working outside the premises.

5.5. Retraining needs

Retraining is a common challenge of diagnosis mechanisms. For the presented naive Bayes classifier this would be required to update the probabilistic models of the indicators if the conditions of the network make them

obsolete. In this respect, conditions that may impact the validity of the models are:

- *Changes in the fault characteristics*, if the conditions related to the failures change significantly from those existing when learning.
- *Variations in the distribution of the UEs*, if the average user distributions vary significantly.
- *Variations in the scenario topology, obstacles, architecture and cell positions*.

The durability of the probabilistic models would be dependent on the extent and variety of the training set used during the learning phase, as well as the dynamic nature of the scenario. However, these challenges are also common to classical diagnosis mechanisms and have been extensively addressed in literature [31]. Here, the use of the proposed contextualized indicators is not expected to introduce additional requirements with respect to classical solutions. From an operational point of view, the update of the models, if necessary, can be performed in background or during low-load periods based on previously recorded cases. Therefore, there should not be challenging cost restrictions introduced by such calculations.

5.6. Computational costs overview

A key point for the application of the presented mechanisms in real time diagnosis is their computational cost and the capabilities of current computing systems to cope with such calculations during online network operation.

One of the main advantages of the presented approach is that the definition of the context mask and the models generation are solely performed during the learning phase. Therefore, the computational requirements for the diagnosis phase are much reduced.

The diagnosis phase is applied once the models and the contextualized KPI values have been already calculated. Its computational cost depends on the number of KPIs selected as input for the classifier as well as the number of failures considered by the diagnosis system. Even if real network monitoring systems contain hundreds/thousands of counters and KPIs, the number of indicators used for diagnosis is commonly much lower. For instance, the classifier in [21] made use of 19 indicators, while the system presented in [11] had just three inputs. If the selected indicators are already calculated by the system, the cost of including more or less of them in the diagnosis phase is low. The addition of one indicator consists in estimating its conditional probabilities and then including it in the product of the other indicators results.

The weight generation would however be the most costly operation in the diagnosis procedure, as it is dependent on the context of each measurement. However, considering that multiple UE indicators would be reported at the same instant (e.g. the UE measurement reports may include both quality and received power measurements), they will also share the same context. Therefore, equal weights may be applied to different measured indicators, reducing the calculation needs. The complexity of the contextualized indicators generation would then be directly

dependent on the number of reports $|R|$ and not on the number of measurements, where each report is defined as a set of *simultaneous values* received for multiple indicators of one UE, e.g. $r(u_i, t_z) = \{m_1(u_i, t_z) \dots m_j(u_i, t_z) \dots\}$. The number of reports in each period would depend on the amount of UEs, the UE reporting frequency and the length of the observation period.

Assuming that the complete diagnosis process is performed at the end of each period (with all the reports gathered in such a period) the complexity would be therefore related to $|R| \cdot \mathcal{O}(W_{calc})$, where $\mathcal{O}(W_{calc})$ is the complexity of calculating the weights applied to each measurement.

With regard to such complexity, service weights defined in terms of a certain characteristic of the terminal would be just computed by comparing the context attribute reported with the defined condition (e.g. throughput below a certain level, a particular serving cell, etc.).

However, location-based weights calculation would be the most complex and costly procedure to be performed. If the location masks are based on defining if a sample belongs to a certain area (e.g. sample located in the cell edge) it would only be required to compute whether its reported position is inside or outside the defined area.

For irregular area shapes, such calculation could be especially costly. However, for the case where areas are defined by Voronoi or following any other regular polygonal form, the complexity of the problem is $\mathcal{O}(|R||V|)$ [32], where V is the number of vertexes of the area. An average of 6 vertexes for each Voronoi area in random plane tessellations is estimated [33], a number that could be a good approximation for general cellular deployments (e.g. in the scenario presented in Fig. 7 the mean is 5 vertexes).

Therefore, assuming polygonal areas, the complexity of the complete diagnosis procedure for one period would imply $\mathcal{O}(|W||R|^3)$. In this expression $|W|$ represents the number of location masks applied to each sample. Even if multiple simplifications and optimizations can be applied for this process [32], the expression clearly indicates the need of minimizing the number of processed measurements. This could be achieved by reducing the observation period, but it would also reduce the available time for the diagnosis. It is also possible to reduce the number of times the weights are recalculated for a certain terminal, if it is assumed that the UE context has remained static (e.g. if the UE has remain essentially static, its location masks values do not need to be recalculated).

6. Performance evaluation

The presented mechanisms are evaluated in the LTE system-level simulator presented in [34], whose general characteristics are summarized in Fig. 6. From the definition of the contextualized indicators multiple options are available for weight definitions, context masks and applications. In this evaluation, different particularizations of the approach would be adopted to provide a glance to the capabilities of the proposed approach.

Here a macrocell environment containing an indoor LTE small cell area is modeled as shown in Fig. 7. Three

Propagation Model	Indoor-indoor	Winner II A1
	Indoor-outdoor	Winner II A2
	Outdoor-outdoor	Winner II C2
	Outdoor-indoor	Winner II C4
Base Station Model	EIRP	3 (small cells) / 43 (macro) dBm
	Directivity	Omni (small) / tri-sector (macro)
	Access	Open (small) / open (macro)
Mobile Station Model	Noise Figure	9dB
	Noise Density	-174dBm/Hz
Traffic Model	Calls	Poisson (avg. 0.43calls/user-h)
	Duration	Exponential (avg. 100 sec)
Mobility Model	Outdoor	3km/h, random direction & wrap-around
	Indoor	Random Waypoint
Service Model	Voice over IP	16 kbps
RRM Model	Full Buffer	
	Bandwidth	1.4 MHz (6 PRBs)
	Access Control	Directed Retry (Threshold=-44dBm)
	Cell Reselection	Criteria S, R
	Handover	Events A3, A5
	Scheduler	Voice: Round-Robin Best Channel Full buffer: Proportional Fair
Time Resolution		100 ms
Diagnosis Algorithm	Epoch Time	60 seconds

Fig. 6. Simulator parameters.

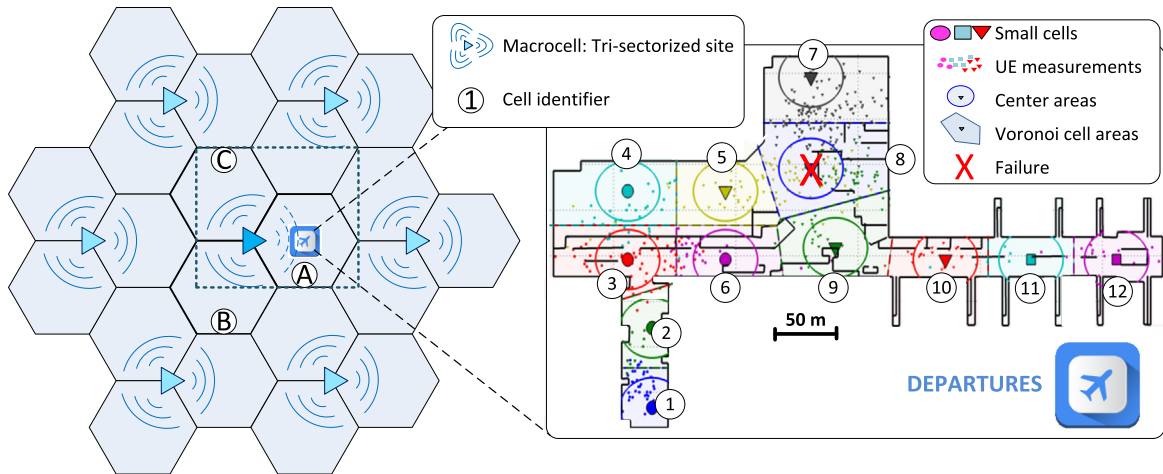


Fig. 7. Simulated airport scenario.

macrocells are placed in the scenario, where the wrap-around technique is used to avoid border effects in the simulation. The indoor scenario has been designed emulating the Málaga airport departures zone. This comprises an area of 200×300 m, with an irregular building plan including boarding gates, security checks and passing boarding bridges. Simulated users move freely in this structure following a random waypoint based model [35], where realistic user pattern concentrations were defined in the security check area, boarding gates, etc.

In order to provide indoor coverage, twelve LTE small cells are deployed in the building following an approximately uniform distribution. This configuration can be considered as following an unplanned approach, as no planning algorithms were used to define the small cell locations. The closest LTE macrocell is located at 376 m to the northwest of the scenario.

This scenario is especially representative for the evaluation of the proposed approach as it includes very different types of areas: open and semi-open ones, shops, corridors and zones full of obstacles and walls. Also, crowded and sparsely populated spots are included. Here, different network failures are simulated. Their impact on UE measurements as well as on the indicators at cell level has been evaluated. The evolution of the system and the users has been simulated with a resolution of 100 ms, where the UE distribution and failure conditions change continuously. The observation period for the indicators calculation is one minute.

The evaluation assessment is focused on the analysis of three key common failures in small cell networks related to variations in cell transmitted power, specifically in their equivalent isotropically radiated power (EIRP). Such failures are generated following the expression:

$$EIRP_{cell}^f = EIRP_{cell}^{normal} + \Delta EIRP_{cell}^f, \quad (8)$$

where the $EIRP_{cell}^f$ of a specific failure f of a faulty cell is equivalent to its normal status average value plus a variation $\Delta EIRP_{cell}^f$. In order to further test the capabilities of the proposed mechanisms, a certain degree of randomness in this parameter is introduced, varying its value each minute following a uniform distribution $\Delta EIRP_{cell}^f = \mathcal{U}(a_f, b_f)$ where the minimum a_f and maximum b_f values depend on each analyzed network state. Hence, the different failures simulated are:

- *Small cell interference*: due to misconfiguration, the cell transmits above its normal level generating interference to its neighbors. For the simulated scenario, the small cells were originally deployed expecting to transmit at the same power (which is a common approach). Here, $\Delta EIRP^f = \mathcal{U}(15, 20)$. Based on commercial small cell characteristics, these values represent a feasible case of EIRP increase, for example, if all the small cells have been configured to transmit at 0 dBm (as in the simulated case), while the misconfigured cell transmits at its maximum power.
- *Macro cell interference*: a signal coming from an external macrocell generates interference inside the indoor scenario, where $\Delta EIRP^f = \mathcal{U}(30, 40)$. This represents realistic values if a previously low powered macrocell starts transmitting at its maximum power. This could also closely reflect the situations where an external repeater or a new macrocell is deployed near the indoor scenario or if relevant structural obstacles (e.g. a building) disappear from its signal propagation path.
- *Cell power degradation*: the cell transmitted power is reduced due to a failure in its RF equipment. It is modeled as a variation in its transmission power of $\Delta EIRP^f = \mathcal{U}(-60, -40)$.

With the inclusion of these randomness margins, the ability of the system to work under different situations and without retraining is also assessed.

6.1. Learning phase

In the simulated scenario, the terminals report multiple measurable indicators and events, such as handovers, received power and quality levels. For the modeled network failures, different measurable variables have been considered, where the channel quality indicator (CQI) [36] is selected as the main source of information about possible channel degradations, as stated in [37]. The CQI provides information on the channel quality experienced by a UE, being directly related to the signal-to-noise-plus-interference ratio of the radio-link.

The CQI has also the advantage of being measured continuously by the terminals, independently of any event. Other counters, such as those based on events (e.g. handovers, drops) are only related to specific events-situations and therefore may not provide continuous information for all positions, being also more vulnerable to the possible

scarcity and random distribution of UE reports in indoor scenarios.

As specific statistics for the CQI, the mean and different Xth-percentile distributions were analyzed. The mean was found to be the most suitable CQI statistic, presenting better stability between different measurement periods under the same fault. In comparison, the 5th percentile statistics have shown very disperse values.

For the classifiers, three inputs have been chosen for each classical or contextualized approach, following the indications described in Section 5.3. For both, the statistical models under each network state (*Normal*, *SC Interference*, *Macro Interference* and *Power degradation*) have been generated. These are based on a training set of 50 periods, being these distributions used to approximate the conditional probabilities for the diagnosis phase.

6.1.1. Classical

The top graph in Fig. 8 shows the temporal evolution of the main CQI-based indicators when cell 8 is the faulty small cell. A failure in that cell is especially significant, as it is located in a semi-open area with also close walls and obstacles.

The indicators are presented for 576 periods of one minute and different network states: normal, macrocell interference, small cell interference and power degradation. Periods when the network is under the same state/fault are placed together as they were simulated contiguously.

The inputs for the diagnosis phase have been chosen based on the indications of Section 5.3, where the most impacted indicators have been selected for each failure:

- *Cell 8 served samples*: Mean CQI of the UEs served by the faulty cell.
- *Cell 7 served samples*: The classic indicator most affected by the macrocell interference.
- *Cells [5, 7, 8, 9]*: Mean CQI of the UEs served by the faulty cell and its adjacent neighbors. It is the indicator most affected by power degradations.

The left side of Fig. 9 shows the statistical models of these indicators (represented by the normalized histogram and its approximate Gaussian distribution) calculated based on the training set for different network states. It can be observed how different causes lead to varied differences between the distributions. For instance, small cell interference situations (*SC Interf.*) clearly impact the CQI distribution of the UEs served by the faulty cell 8. In fact, a simple threshold (e.g. in CQI = 10) could serve to identify if the CQI value corresponds to small cell interference. However, the distributions for the macro interference case (*Macro Interf.*) and the power degradation failure (*Power degr.*) present overlapping between them and with the normal state, which would lead to erroneous classifications in the diagnosis phase.

6.1.2. Contextualized

Given the analyzed issues, UE location information is the main context attribute to be taken into account for the diagnosis. The cell area is defined as the power-

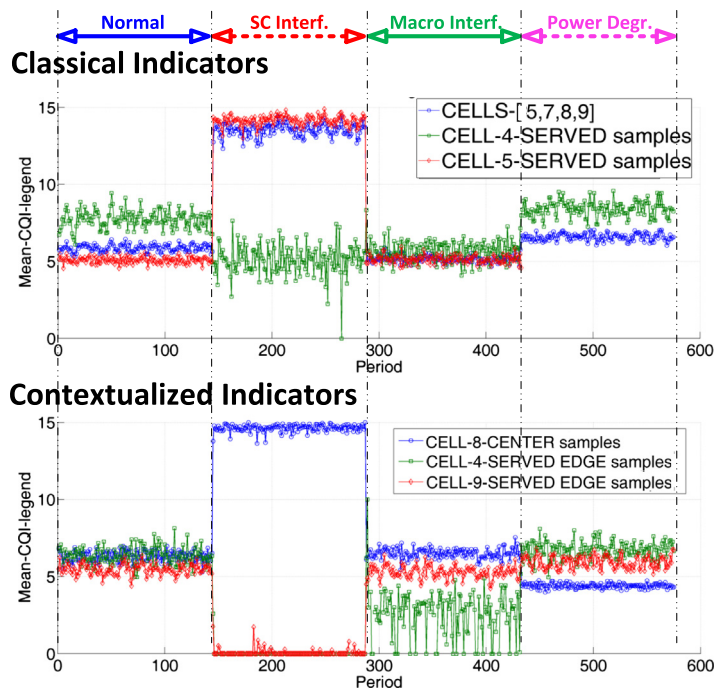


Fig. 8. Evolution of classic and contextualized CQI indicators.

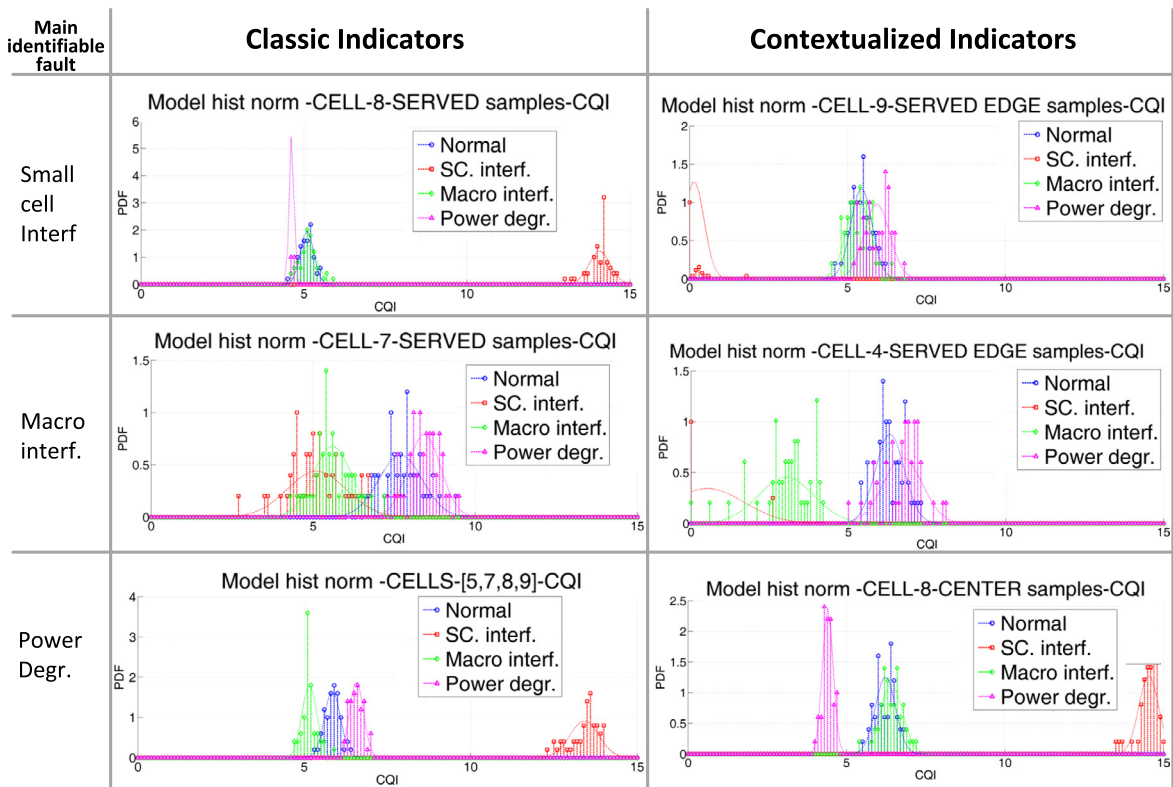


Fig. 9. Indicators statistical models.

diagram based area of each cell. The cell center is established as the circular area surrounding a specific small cell with a radius of the 75% of the shortest distance between the small cell position and the closest neighboring power-diagram area. The cell edge is defined as the coronal area surrounding a cell formed by its Voronoi area discarding the cell center.

As previously stated, these Voronoi-based areas have the advantage of not requiring any particular information about the scenario besides the relative location of each small cell with respect to its neighbors and their transmitted power. Also, they allow a faster calculation of a point belonging or not to a specific area. A Voronoi tessellation would acceptably approximate coverage areas in line of sight scenarios with equal transmitted power for all small cells. This approach however may introduce inaccuracies in scenarios including obstacles, walls, etc. For the analyzed scenario, these are considered a good approximation. This can be observed in Fig. 7, where in the airport scenario, the different plotted UEs are served by the base stations in good correspondence with their Voronoi areas. Except for cell 8, whose transmitted power is degraded in that situation, the marks and colors associated to the serving cell of the UEs coincide mainly with the tessellation.

The lack of UE measurements cannot be directly associated with a failure as it may be dependent of the real absence of users and/or cell monitoring issues. For these situations, the location masks are a powerful tool for obtaining contextualized indicators for the failure-affected areas, even when the cell is not able to report UE measurements. In this way, edge masks are applied in combination with service masks for the adjacent neighbors. However, the cell center mask for the possible faulty cell is applied without service mask to avoid lack of data in case the faulty cell is too degraded to serve any UE.

The bottom graph in Fig. 8 shows the temporal evolution of the most important contextualized indicators. Again, those more impacted by each failure are selected. The impact of the power degradation failure can be observed in the *Cell-8-CENTER samples* indicator. Its profile shows a clear reduction in the CQI values, making it the most suitable indicator for identifying the cause. Additionally, the most important served edge indicators are represented. As expected, *Cell-4-SERVED EDGE samples* shows the highest degradation for macro interference. Finally, *Cell-9-SERVED EDGE samples* is assumed to be one of the most affected indicators by the small cell interference generated by its adjacent cell 8.

The statistical models for these indicators are represented on the right side of Fig. 9. Compared to their classical counterparts, the contextualized indicators present a clearer distinction between the modeled network states, which should lead to a better performance in the diagnosis of network failures.

6.2. Diagnosis phase

The indicators included in Fig. 9 are selected as inputs for the naive Bayes classifier used in the diagnosis phase, for both classic and contextualized indicators.

For the classifier, prior probabilities of each network state have to be defined by human experts or by analyzing the occurrence of each cause in previously recorded data. In order to properly evaluate the capabilities of the proposed mechanisms, prior distributions are considered equal, so the results are not dependent on the quality of the prior probability estimation. The conditional probabilities are calculated based on the Gaussian approximate models generated during the learning phase.

The performance of the diagnosis results is measured in terms of the capability and accuracy for identifying each cell condition, as presented in Fig. 10. This is evaluated by three main figures of merit:

- *Type I error rate* or false positive ratio: the percentage of erroneous positives obtained for a cause with respect to the total number of periods where the cause is not really present.
- *Type II error rate* or false negative ratio: the percentage of periods where the real cause is not diagnosed over the number of periods where it is present.
- *No data rate*: defined as the percentage of periods where diagnosis could not be performed. This can be due to the absence of UE measurements meeting the context masks conditions. As presented in Section 4.3, the lack of a contextualized indicator input can lead to not providing any diagnosis depending on the technique applied (fallback, no diagnosis or discard KPI).

In terms of data scarcity, in the presented simulation, *CELL-4-SERVED EDGE* indicator (generated by combining the location mask of the cell 4 edge and the service mask of being served by cell 4) is the only one that includes some periods with no samples. In particular, there were 52 periods without values (in a total of 576 simulated periods), where such intervals are coincident with the small cell interference situation and therefore are caused by cell 8 serving the users located in the cell 4 edge due to its increased transmitted power. Thus, the contextualized KPI cannot be calculated in such periods. In order to address this issue, the three main approaches presented in Section 4.3 are applied. Particularizing, the *fallback* technique is implemented using the classic indicator *CELL-7-SERVED SAMPLES* as a substitute of *CELL-4-SERVED EDGE* for periods where the contextualized indicator cannot be calculated.

These approaches are compared with the classic solution, and the results are presented in Fig. 10. The left side of this figure contains the bar graph presenting the type I, type II and no data rates for each network state and the classical and contextualized indicators approaches.

On the one hand, both classic and contextualized indicators diagnosis obtain perfect performance for the small cell interference cause. This is expected from the large statistical deviation generated for such failure in both classical and contextualized indicators.

On the other hand, contextualized indicators greatly improve the accuracy of the diagnosis of the other three network conditions. Their capabilities especially impact the situations where a greater statistical difference is achieved in comparison to the classical approach, e.g. for

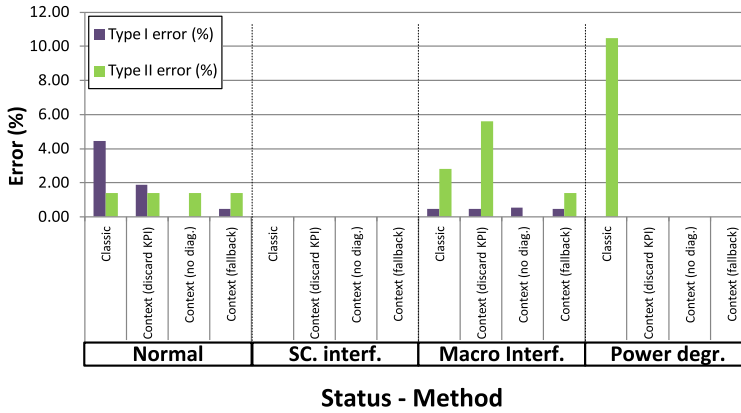


Fig. 10. Diagnosis evaluation per each method and case.

the diagnosis of the normal status and the power degradation failure. For the normal state, the type I error is reduced very significantly from the 4.43% to the 0.47% (fallback). For the power degradation failure, any contextualized approach achieves zero error in comparison to the 10.49% of the classical case. Additionally, the defined fallback technique provides diagnosis for all periods while only slightly degrading the performance in comparison to the *no diagnosis* solution.

In order to have a summarized view of the network performance, Fig. 11 shows the total diagnosis error rate, measured as the percentage of samples incorrectly classified over the total number of diagnosed periods, independently of the particular cause. The periods where diagnosis is not performed due to lack of data are not included in the ratio. Instead, those periods are represented by the *no data rate* bar, defined as the percentage of samples where the mechanisms do not classify the network status. Here, it is shown how the context *no diagnosis* is the one providing the best accuracy, with only a 0.4% of error at the cost of not providing any classification for the 12% of the periods. On the other hand, the fallback approach gives a slightly higher error but still it provides an accuracy 5 times lower than the one given by the classical indicators.

Finally the proposed mechanisms are applied to the same scenario and different faulty cells. In particular, small

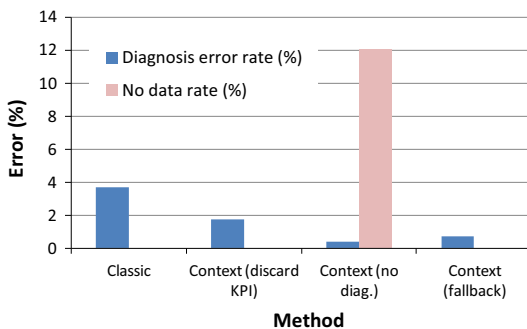


Fig. 11. Diagnosis evaluation for the different methods and faulty cell 8.

cell interference and power degradation issues are emulated in cells 4, 5, 6, 7, 8, 9 and 10. For each case, the indicators are particularized for the corresponding faulty cell. For the contextualized approach, the indicators used for diagnosis are the faulty cell center CQI and the adjacent neighbor served edge CQI.

The results are presented in Fig. 12. The table includes the diagnosis error rate for the different techniques, as well as the *no data rate* for the context (*no diagnosis*) approach. Here, it is shown how for the main cells of the building, the proposed mechanisms achieved much better performance than the classical approach.

This is especially interesting for the case of cell 7, where a unique adjacent cell is available to support the diagnosis. In this case, the classic mechanism has a very high diagnosis error rate (11.89%) while the contextualized approaches maintain good performance.

For the faulty cell 10 case as well as for cell 6, the contextualized indicators do not provide a very high advantage over the classical one, being in fact inferior for the cell 6 case. This is given by the particular location of these cells, which makes their small cell interference failure easy to differentiate from the macro interference one: as these faulty cells are isolated from the rest of the network cells, their excessive transmission power does not affect the cell 7 CQI values used for diagnosis in the classical approach. In the implementation of the system, these situations can be automatically detected based on the training data, making

Faulty cell	Diagnosis error rate (%)				No data rate (%)
	Classic	Context (discard KPI)	Context (no diag.)	Context (fallback)	Context (no diag.)
Cell 4	3.15	30.42	1.24	2.62	29.55
Cell 5	2.97	2.10	0.60	0.70	12.06
Cell 6	0.70	4.02	2.58	2.62	5.07
Cell 7	11.89	1.92	1.09	1.05	3.50
Cell 8	3.67	1.75	0.40	0.70	12.06
Cell 9	8.74	2.62	0.72	0.70	2.97
Cell 10	14.16	13.11	12.77	12.41	2.80

Fig. 12. Analysis of the diagnosis error and no data rate for different faulty cells.

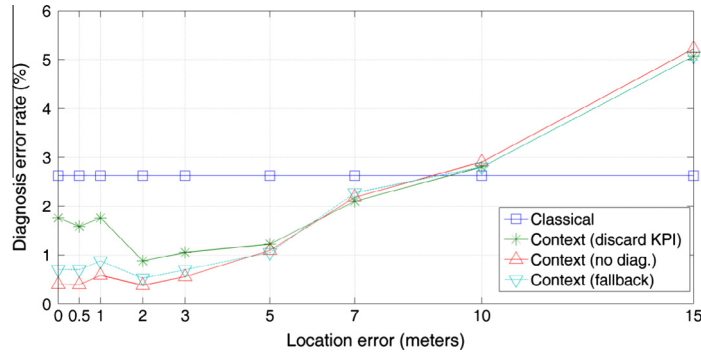


Fig. 13. Diagnosis accuracy given the location error.

use of the classical indicators when the use of contextualized ones is unnecessary.

6.3. Impact of localization error

An important consideration for the applicability of location based context masks is its robustness to errors in the UE positions. A priori, this would be particularly dependent on the size of the considered areas.

To evaluate this point, errors in the localization sources are modeled in the simulated scenario. To do so, a random error is aggregated to each known position of the UEs before the sample weights are calculated. Such an error is modeled as a normal Gaussian random variable added to the components of the UE position:

$$\begin{cases} e_x^m = N(\mu, \sigma) \\ e_y^m = N(\mu, \sigma) \end{cases} \quad (9)$$

where e_x^m and e_y^m are the Gaussian error components aggregated to the vertical and horizontal axis coordinates respectively. μ equals 0 for all cases while the standard deviation is in the range $\sigma = \{0, 0.5, 1, 2, 3, 5, 7, 10, 15\}$ m. This is in accordance to real indoor localization systems, whose error ranges from dozens of centimeters to a few meters depending on the technique and the conditions of the environment [23–25].

Fig. 13 shows the results of the analysis for the faulty cell 8 cases, where the diagnosis error rate of the algorithms is represented given the standard deviation of the introduced location error.

The figure shows how the use of contextualized indicators keeps providing better results than the classical one even for error values as high as 7 m. The contextualized methods even have half the error of the classical one for a localization inaccuracy of 5 m, showing a high level of resiliency against imprecision in the available UE positions.

7. Conclusions

The present work has defined a novel approach for network failure diagnosis, where network diagnosis is performed by processing newly defined contextualized indicators. These are constructed combining UE measurements

of different radio indicators together with context information, such as the location of the terminal. Based on the novel application of samples weights, contextualized indicators allow a smooth integration in existing diagnosis schemes.

The comprehensive mathematical fundamentals for the proposed approach have been presented: from the application of weight samples to the application of contextualized statistics. Additionally, the concept of context masks has been defined, consisting in sets of sample weights based on different context variables. These masks can be applied to the collected UE measurements to generate distinct contextualized indicators. The implications of implementing the approach in real systems have been also assessed.

The capabilities of such mechanisms have been evaluated by an LTE system-level simulator modeling a small cell network deployment located in a large indoor scenario. The diagnosis of different network failures has been performed based on classical and contextualized indicators. UE context, in particular serving cell and location masks, is used to improve the analysis of the network. The results show a relevant increase in accuracy by the proposed system in comparison with classical approaches. Also, additional analysis on the impact of UE location errors shows the resilience of the approach against high levels of positioning inaccuracy.

Acknowledgments

This work has been partially funded by the Spanish Ministry of Economy and Competitiveness within the National Plan for Scientific Research, Technological Development and Innovation 2008–2011 and the European Development Fund (ERDF), within the MONOLOC project (IPT-430000-2011-1272). This work has been also partially supported by the Junta de Andalucía (Proyecto de investigación de Excelencia P12-TIC-2905).

References

- [1] NGMN Alliance. <<http://www.ngmn.org/>> (accessed 19.11.14).
- [2] 3GPP. <<http://www.3gpp.org/>> (accessed 19.11.14).
- [3] 3GPP, Telecommunication Management; Principles and High Level Requirements, TS 32.101, 3rd Generation Partnership Project (3GPP), 2012.

- [4] I. Frank, N. Magid Associates, Smartphones and Tablets: The Heartbeat of Connected Culture, 2013. <<http://magid.com/sites/default/files/pdf/20130930MagidMobileStudyPreview.pdf>>.
- [5] A.K. Dey, Understanding and using context, *Personal Ubiquitous Comput.* 5 (1) (2001) 4–7.
- [6] Small Cell Forum. <<http://www.smallcellforum.org>> (accessed 19.11.14).
- [7] R. Barco, P. Lázaro, P. Muñoz, A unified framework for self-healing in wireless networks, *IEEE Commun. Mag.* 50 (12) (2012) 134–142.
- [8] J. Ramiro, K. Hamied, Self-Organizing Networks (SON): Self-Planning, Self-Optimization and Self-Healing for GSM, UMTS and LTE, first ed., Wiley Publishing, 2012.
- [9] S. Hämläinen, H. Sanneck, C. Sartori, LTE Self-Organising Networks (SON): Network Management Automation for Operational Efficiency, Wiley, 2011.
- [10] M. Asghar, S. Hamalainen, T. Ristaniemi, Self-healing framework for LTE networks, in: 2012 IEEE 17th International Workshop on Computer Aided Modeling and Design of Communication Links and Networks (CAMAD), 2012, pp. 159–161.
- [11] P. Szilagyi, S. Novaczki, An automatic detection and diagnosis framework for mobile communication systems, *IEEE Trans. Network Service Manage.* 9 (2) (2012) 184–197.
- [12] S. Novaczki, An improved anomaly detection and diagnosis framework for mobile network operators, in: 2013 9th International Conference on the Design of Reliable Communication Networks (DRCN), 2013, pp. 234–241.
- [13] W. Hapsari, A. Umesh, M. Iwamura, M. Tomala, B. Gyula, B. Sebire, Minimization of drive tests solution in 3gpp, *IEEE Commun. Mag.* 50 (6) (2012) 28–36.
- [14] 3GPP, 3rd Generation Partnership Project; Technical Specification Group Radio Access Network; Universal Terrestrial Radio Access (UTRA) and Evolved Universal Terrestrial Radio Access (E-UTRA); Radio measurement collection for Minimization of Drive Tests (MDT); Overall description; Stage 2 (Release 12), TS 37.320, 3rd Generation Partnership Project (3GPP), March 2014.
- [15] F. Chernogorov, J. Turkka, T. Ristaniemi, A. Averbuch, Detection of sleeping cells in LTE networks using diffusion maps, in: 2011 IEEE 73rd Vehicular Technology Conference (VTC Spring), 2011, pp. 1–5.
- [16] C. Baladron, J. Aguiar, B. Carro, L. Calavia, A. Cadenas, A. Sanchez-Esguevillas, Framework for intelligent service adaptation to user's context in next generation networks, *IEEE Commun. Mag.* 50 (3) (2012) 18–25.
- [17] S. Fortes, A. Aguilar-García, R. Barco, F. Barba, J. Fernández-Luque, A. Fernández-Durán, Management architecture for location-aware self-organizing lte/lte-a small cell networks, *IEEE Commun. Mag.* 53 (1) (2015) 294–302.
- [18] S. Fortes, A. Aguilar-García, R. Barco, A. Garrido, J. Fernández-Luque, Context-aware self-healing in LTE small-cell networks, *IEEE Veh. Technol. Mag.* (submitted for publication).
- [19] R. Groves, F. Fowler, M. Couper, J. Lepkowski, E. Singer, R. Tourangeau, *Survey Methodology*, Wiley Series in Survey Methodology, John Wiley & Sons, 2009.
- [20] I. Narsky, F.C. Porter, *Density Estimation*, Wiley-VCH Verlag GmbH and Co. KGaA, 2013. Ch. 5, pp. 89–120.
- [21] R. Barco, V. Wille, L. Díez, System for automated diagnosis in cellular networks based on performance indicators, *Euro. Trans. Telecommun.* 16 (5) (2005) 399–409.
- [22] H. Zhang, The optimality of naive bayes, in: FLAIRS Conference, 2004, pp. 562–567.
- [23] M. Dakkak, A. Nakib, B. Daachi, P. Siarry, J. Lemoine, Indoor localization method based on RTT and AOA using coordinates clustering, *Comput. Networks* 55 (8) (2011) 1794–1803.
- [24] R.S. Campos, L. Lovisolo, M.L.R. de Campos, Wi-fi multi-floor indoor positioning considering architectural aspects and controlled computational complexity, *Exp. Syst. Appl.* 41 (14) (2014) 6211–6223.
- [25] M. Stella, M. Russo, D. Begušić, Fingerprinting based localization in heterogeneous wireless networks, *Exp. Syst. Appl.* 41 (15) (2014) 6738–6747.
- [26] 3GPP, 3rd Generation Partnership Project; Technical Specification Group Services and System Aspects; Functional Stage 2 Description of Location Services (lcs) (release 12), TS 23.271, 3rd Generation Partnership Project (3GPP), December 2013.
- [27] R. Barco, P. Lázaro, V. Wille, L. Díez, S. Patel, Knowledge acquisition for diagnosis model in wireless networks, *Exp. Syst. Appl.* 36 (3) (2009) 4745–4752.
- [28] F. Aurenhammer, Power diagrams: properties, algorithms and applications, *SIAM J. Comput.* 16 (1) (1987) 78–96.
- [29] P. Kyösti, J. Meinilä, L. Hentilä, X. Zhao, T. Jämsä, C. Schneider, M. Narandzić, M. Milojević, A. Hong, J. Ylitalo, V.-M. Holappa, M. Alatosava, R. Bultitude, Y. de Jong, T. Rautiainen, WINNER II Channel Models, Tech. rep., EC FP6, September 2007.
- [30] M. Molina-García, J. Calle-Sánchez, J.I. Alonso, A. Fernández-Durán, F.B. Barba, Enhanced in-building fingerprint positioning using femtocell networks, *Bell Labs Tech. J.* 18 (2) (2013) 195–211.
- [31] W.P. Gajewski, Adaptive Naive Bayesian anti-spam engine, *Int. J. Inf. Technol.* 3 (2006) 153–159 (CERN-OPEN-2007-011. 3), 7 p..
- [32] K. Hormann, A. Agathos, The point in polygon problem for arbitrary polygons, *Comput. Geom. Theory Appl.* 20 (3) (2001) 131–144.
- [33] K.A. Brakke, Statistics of random plane voronoi tessellations, Department of Mathematical Sciences, Susquehanna University (Manuscript 1987a).
- [34] J.M. Ruiz-Avilés, S. Luna-Ramírez, M. Toril, et al., Design of a computationally efficient dynamic system-level simulator for enterprise LTE femtocell scenarios, *J. Electr. Comput. Eng.* 2012 (2012) 14 pages, Article ID: 802606, <http://dx.doi.org/10.1155/2012/802606>.
- [35] D. Johnson, D. Maltz, Dynamic source routing in ad hoc wireless networks, in: T. Imielinski, H. Korth (Eds.), *Mobile Computing, The Kluwer International Series in Engineering and Computer Science*, vol. 353, Springer, US, 1996, pp. 153–181.
- [36] 3GPP, Universal Mobile Telecommunications System (UMTS); Physical Layer Procedures (FDD) (3GPP TS 25.214 version 12.0.0 release 12), TS 25.214, 3rd Generation Partnership Project (3GPP), September 2014.
- [37] S. Novaczki, P. Szilagyi, Radio channel degradation detection and diagnosis based on statistical analysis, in: 2011 IEEE 73rd Vehicular Technology Conference (VTC Spring), 2011, pp. 1–2.



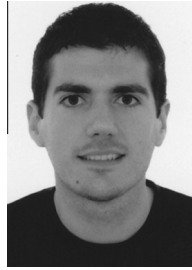
Sergio Fortes received his M.Sc. degree in Telecommunication Engineering from the University of Málaga (Spain) in 2008. He began his career in the field of satellite communications being through different positions in main European space agencies: DLR, CNES and ESA; where he participated in various research activities, mainly on the analysis and development of MAC/PHY layers for aeronautical satellite communications. In 2010, he joined the satellite operator Avanti Communications, where he acted as consultant and coordinator of different research projects with the European Space Agency and other partners. In 2012 he joined the Communications Engineering department at the University of Málaga, where he is currently pursuing his Ph.D. focused on the development of innovative SON techniques for mobile networks.



Raquel Barco holds a M.Sc. and a Ph.D. in Telecommunication Engineering. She has worked at Telefonica in Madrid (Spain) and at the European Space Agency (ESA) in Darmstadt (Germany). From 2000 to 2003, she worked part-time for Nokia Networks. In 2000 she joined the University of Málaga, where she is currently Associate Professor. Her research interests include satellite and mobile communications, mainly focusing on Self-Organizing Networks.



Alejandro Aguilar-García graduated in Telecommunications Engineering in 2010 at the University of Málaga, in the fields of Telematics and Communications. He improved his mobile communications skills coursing an Expert Mobile Communications Course in 2009. He started his career at Sony European Technology Centre in the Speech and Sound Group, participating on an existing video classification system based on audio and image features. He is currently working towards a Ph.D. developing novel SON mechanisms for small-cells in mobile networks at the Communications Engineering Department at the University of Málaga.



Pablo Muñoz received his M.Sc. and Ph.D. degrees in Telecommunication Engineering from the University of Málaga (Spain) in 2008 and 2013, respectively. From 2009 to 2013, he was a Ph.D. Fellow in self-optimization of mobile radio access networks and radio resource management. Upon completing his Ph.D., he has continued his career at the University of Málaga as a research assistant within an R&D contract with Optimi-Ericsson focusing on Self-Organizing Networks. In 2014 he held a postdoc position granted by the Andalusian Government in support of research and teaching.